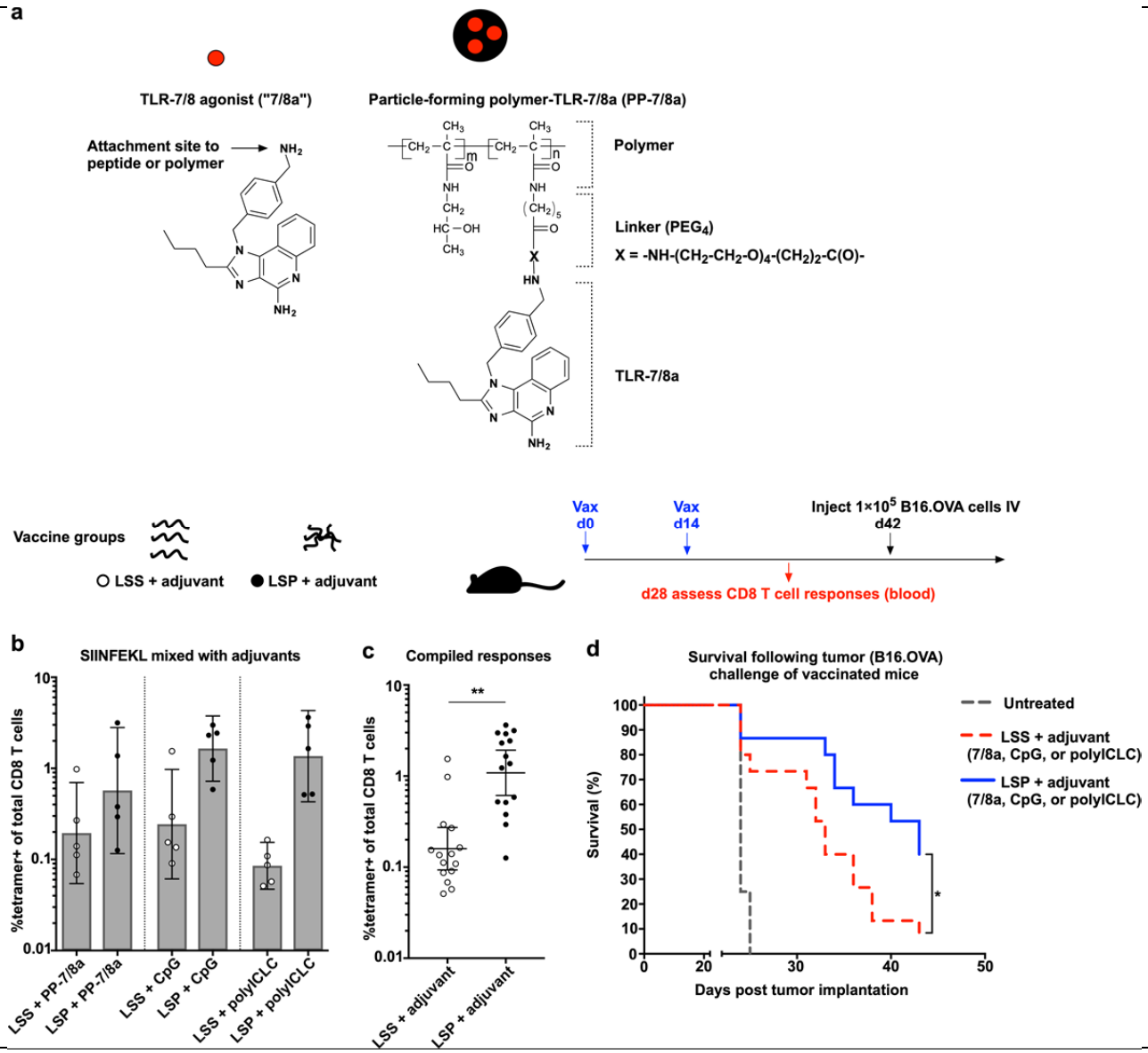

Supplementary Figure 1

Efficiency of CD8 T cell induction depends on LP physical form.

(**a**) Chemical structures of both the imidazoquinoline-based Toll-like receptor-7 & -8 agonist (TLR-7/8a) that was linked to the SIINFEKL LPs (LSS-7/8a and LSP-7/8a) and the particle-forming polymer-TLR-7/8a (PP-7/8a). (**b**–**d**) C57BL/6 mice (*n* = 5 per group) were injected subcutaneously with LSS or LSP admixed with either PP-7/8a, CpG or polyICLC at days 0 and 14. (**b**) Tetramer+ CD8 T cell responses were assessed by flow cytometry on day 28 for each adjuvant. (**c**) Responses from panel (**b**) grouped according to antigen physical form (LSS or LSP). (**d**) C57BL/6 mice vaccinated with either LSS or LSP mixed with adjuvant (*n* = 15 per group) were challenged with B16.OVA on day 42 and assessed for survival. Data on log scale are reported as geometric mean with 95% c.i. Comparison of multiple groups for statistical significance was determined using Kruskal-Wallis with Dunn's correction; statistical significance of survival was determined using Log-rank test; ns = not significant, $*P < 0.05$, $**P \leq 0.01$.

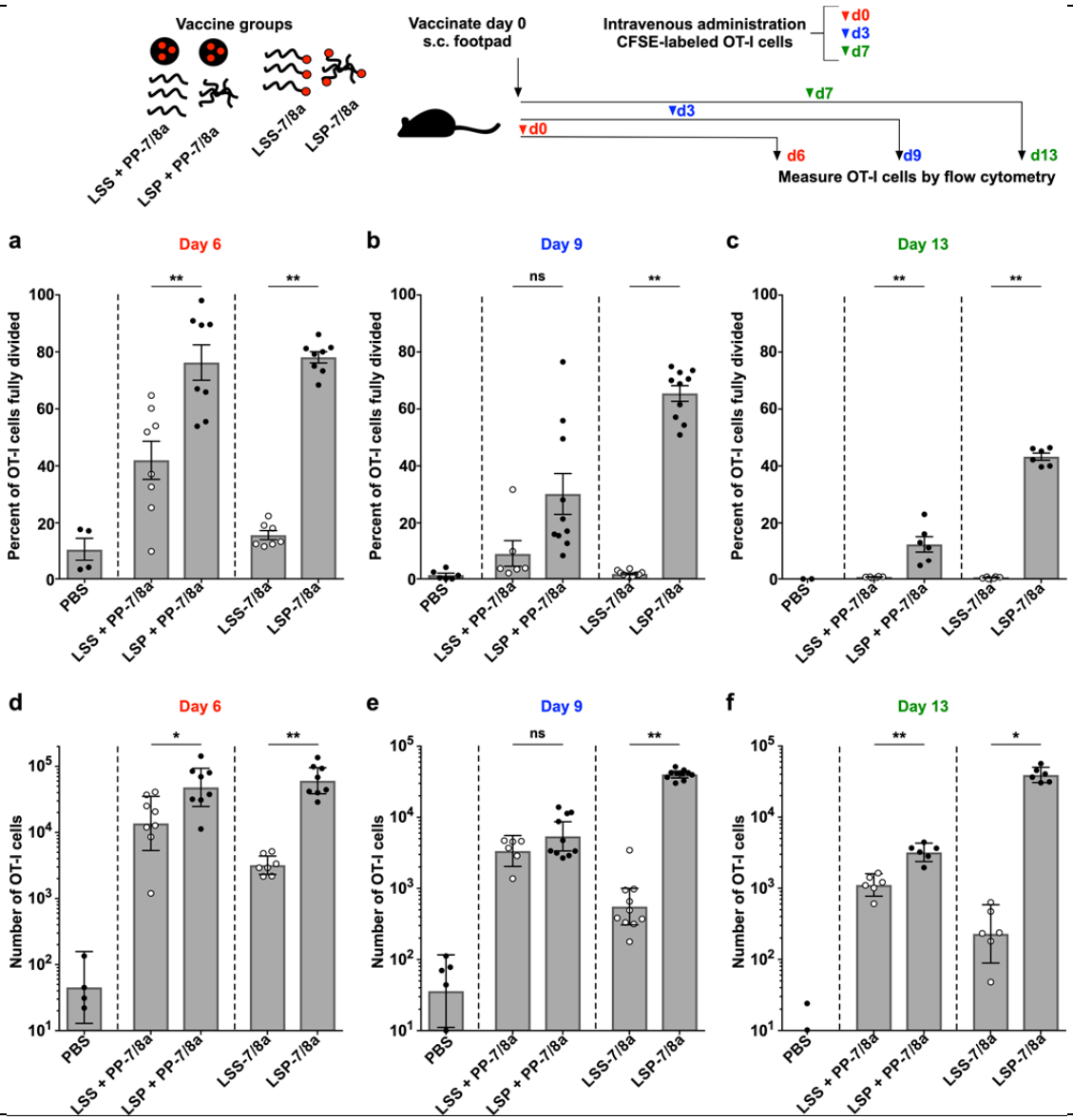

Supplementary Figure 2

Particulate LPs prolong antigen presentation *in vivo* leading to higher frequencies of antigen-specific CD8 T cells.

(**a**–**f**) Three separate cohorts of C57BL/6 mice (n = 5–8 per group per time point) were injected subcutaneously with LSS or LSP, either admixed with PP-7/8a or covalently linked to TLR-7/8a (LSS-7/8a and LSP-7/8a). CFSE-labeled OT-I cells were then administered intravenously to each cohort on day 0, 3 or 7. Six days after receiving the OT-I cells, the percent of OT-I cells that fully divided (**a**–**c**) and total number of OT-I cells (**d**–**f**) were determined by flow cytometry. Data on linear scale are reported as mean ± s.e.m; data on log scale are reported as geometric mean with 95% c.i. Comparison of multiple groups for statistical significance was determined using Kruskal-Wallis with Dunn's correction; ns = not significant, *P < 0.05, **P ≤ 0.01.

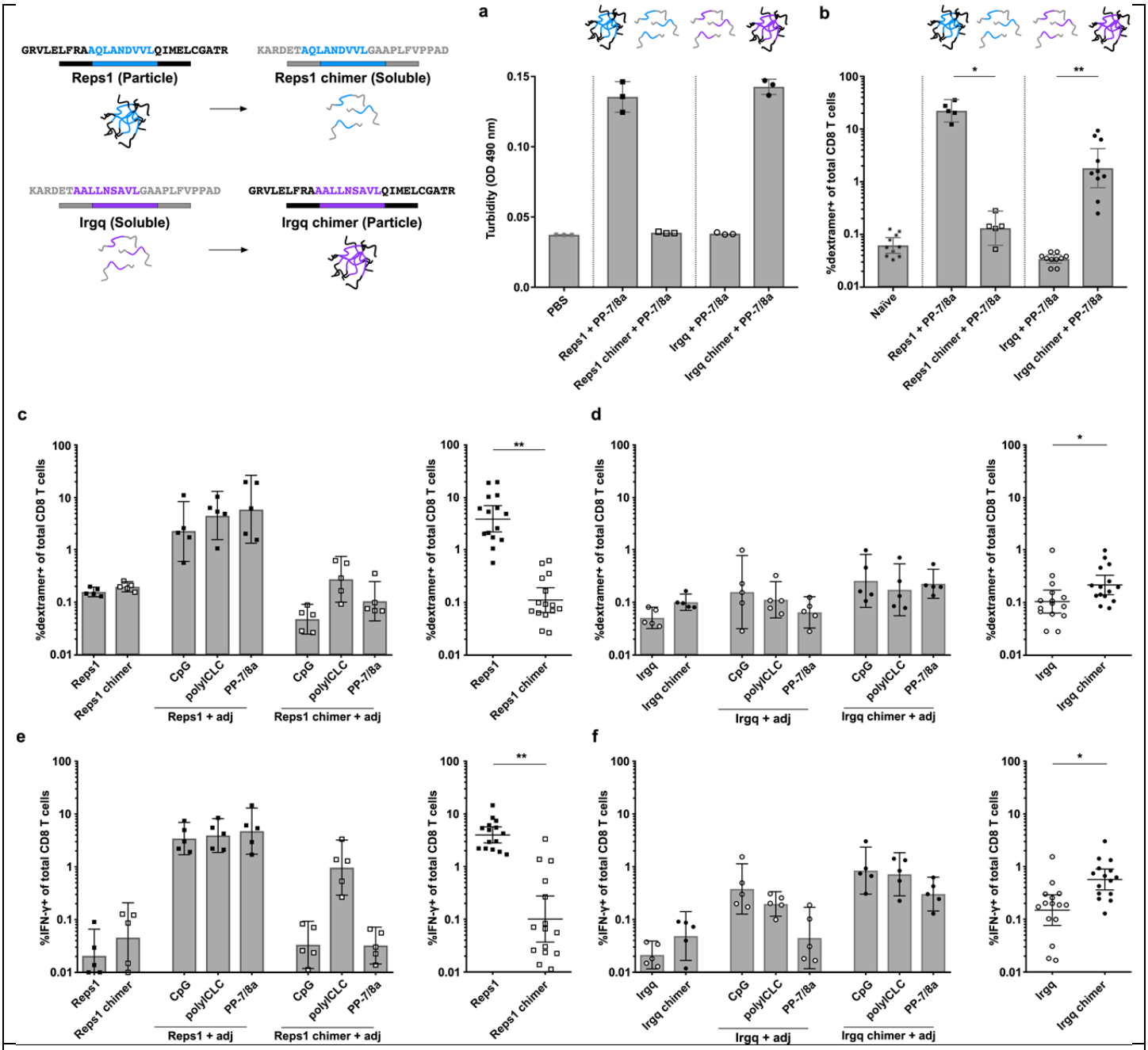

Supplementary Figure 3

Particulate but not soluble neoantigen LPs induce CD8 T cell responses.

(**a**–**f**) The amino acid residues flanking the minimal epitopes of Reps1 (AQLANDVVL) and Irgq (AALLNSAVL) neoantigens were exchanged to generate Reps1 and Irgq chimers. (**a**) Turbidity, as measured by the absorbance (OD, arbitrary units) at 490 nm, was used to assess whether different LPs aggregate (OD > 0.05) or are soluble (OD ≤ 0.05) in aqueous solution. (**b**–**f**) Native and chimeric forms of Reps1 and Irgq LP neoantigens were admixed with different adjuvants (*i.e.* PP-7/8a, CpG or polyICLC) and subcutaneously administered to C57BL/6 mice (n = 5–10 mice per group) on days 0 and 14 and CD8 T cell responses were assessed by either (**b**–**d**) dextramer staining (AQLANDVVL-H-2D^b or AALLNSAVL-H-2D^b) or (**e**,**f**) IFN-γ intracellular cytokine staining of blood on day 28. Data on linear scale are reported as mean ± s.e.m; data on log scale are reported as geometric mean with 95% c.i. Comparison of multiple groups for statistical significance was determined using Kruskal-Wallis with Dunn's correction; Mann-Whitney test was used to assess significance for comparison of compiled responses in figure panels **c**–**f**; ns = not significant, *P < 0.05, **P ≤ 0.01.

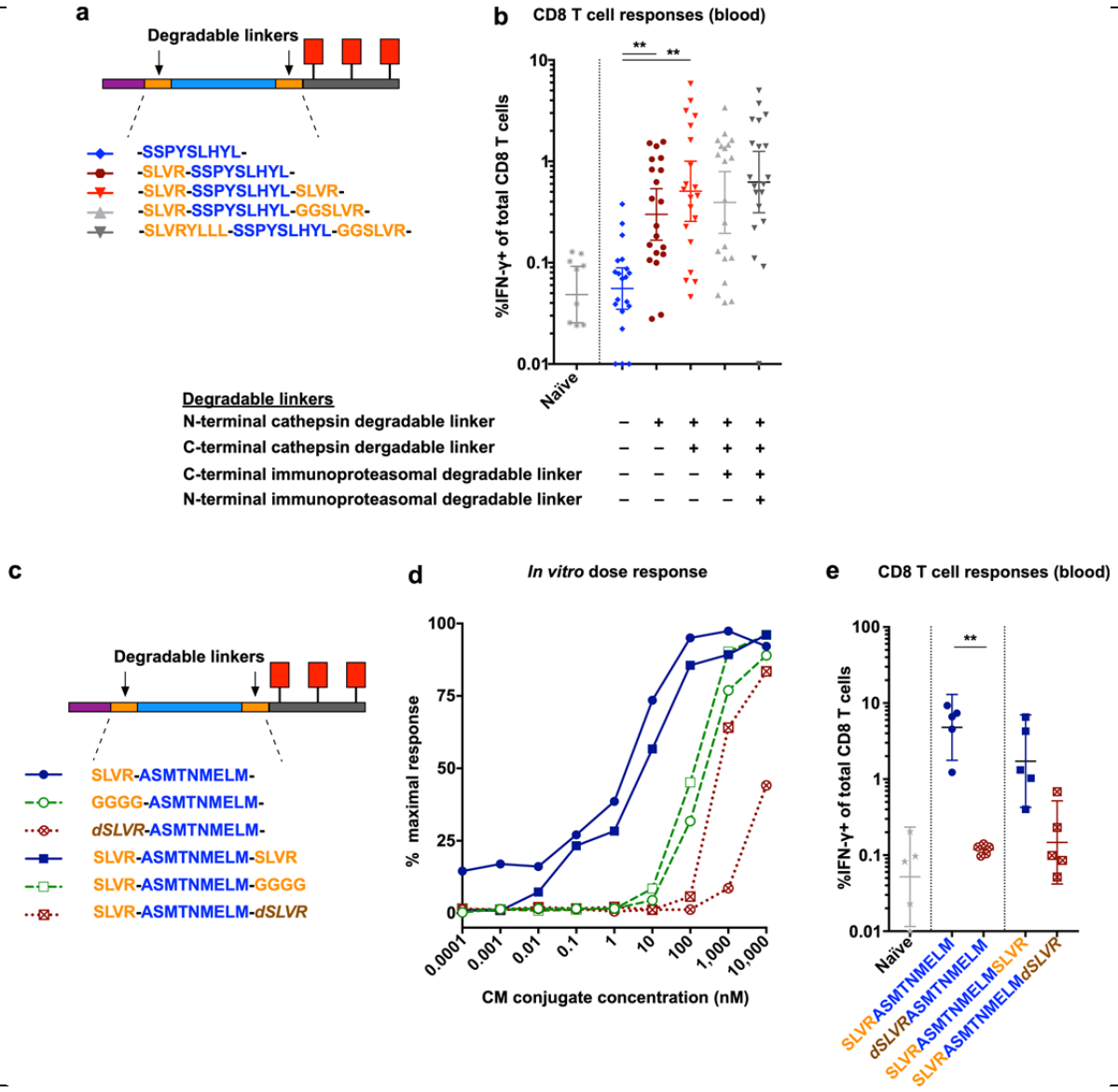

Supplementary Figure 4

Effect of enzyme degradable linker composition on antigen presentation and CD8 T cell priming.

(**a**,**b**) An MHC-I (H-2D^b)-restricted epitope (SSPYSLYHL) from the MC38 tumor cell line-derived neoantigen, Cpne1, was linked at the N-terminus to a charge modifying group either directly or through enzyme (cathepsin, or cathepsin and proteasome) degradable peptide linkers, and at the C-terminus to an oligo-7/8a either directly or through enzyme (cathepsin, or cathepsin and proteasome) degradable linkers. (**b**) C57BL/6 mice (*n* = 20 per group) were injected subcutaneously with Cpne1 (SSPYSLYHL) as CM conjugates of varying degradable linker composition on day 0 and CD8 T cell responses from blood were assessed by intracellular cytokine staining on day 7. Addition of cathepsin degradable linkers significantly increased the CD8 T cell response, which was not further increased with addition of linkers that are also recognized by the proteasome. (**c**–**e**) An MHC-I (H-2D^b)-restricted epitope (ASMTNMELM) from the MC38 tumor cell line neoantigen, Adpgk, was prepared as either a CM conjugate with a cathepsin degradable linker (SLVR) at the N-terminus or at both the N- and C-termini; alternatively, the cathepsin degradable linker was replaced with a non-specific sequence (GGGG) or with D amino acids (dSLVR). (**d**) *In vitro* antigen presentation as assessed by titrating the indicated CM conjugates with ASMTNMELM-specific CD8 T cells and measuring the IFN-γ response by intracellular cytokine staining. (**e**) *In vivo* priming of CD8 T cells by the indicated CM conjugates. Note: use of the D-chirality amino acid (*i.e.* dSLVR) abrogates activity. Data on log scale are reported as geometric mean with 95% c.i. Comparison of multiple groups for statistical significance was determined using Kruskal-Wallis with Dunn's correction; ns = not significant, **P* < 0.05, ***P* ≤ 0.01.

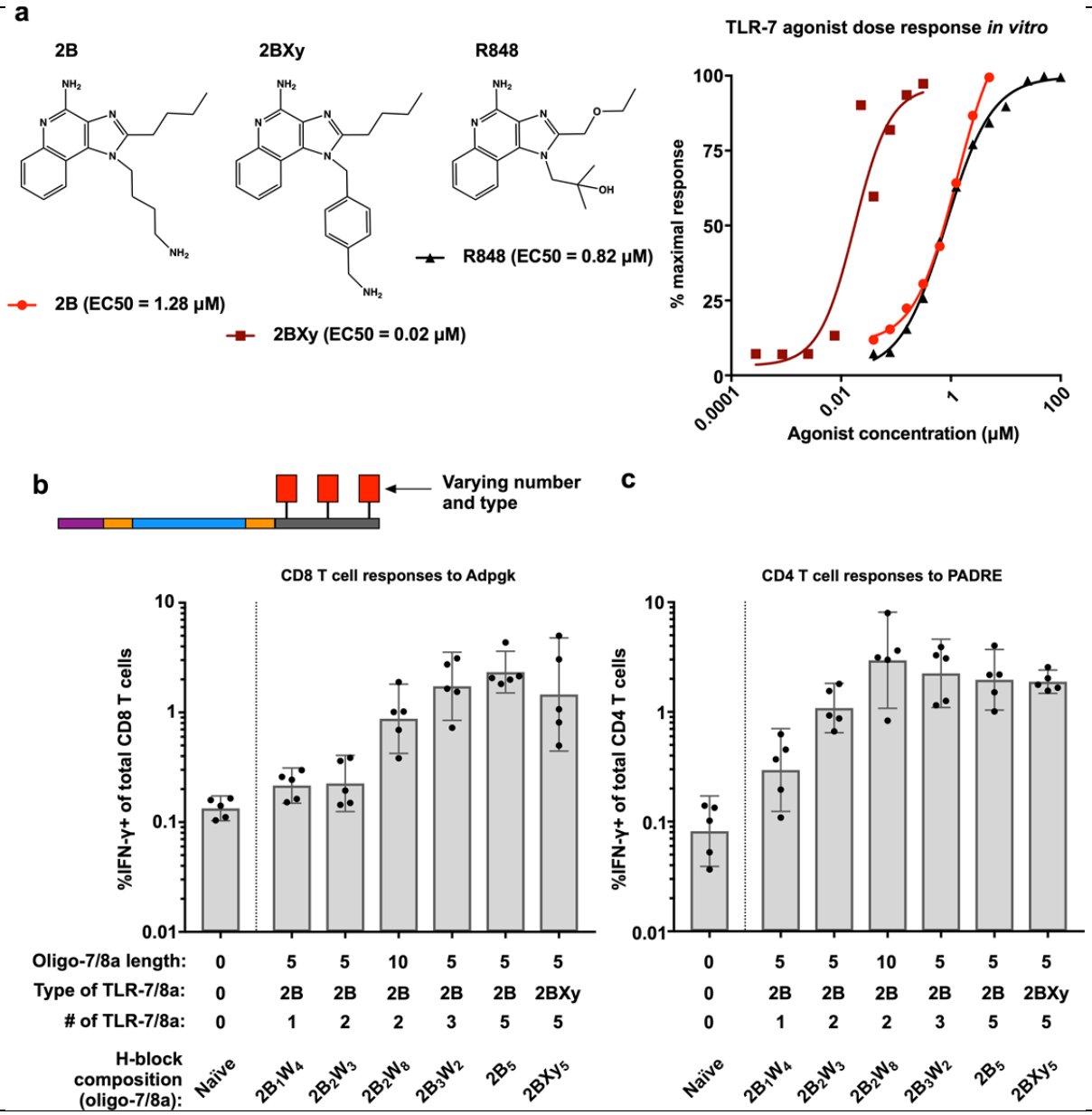

Supplementary Figure 5

Impact of the number and type of TLR-7/8a on T cell responses.

(**a**) Chemical structures and *in vitro* dose response curves for the conjugatable imidazoquinoline TLR-7/8 agonists "2B" (EC_{50} = 1.28 μM) and "2BXy" (EC_{50} = 0.02 μM). Potency was determined via a colorimetric reporter assay by incubating different concentrations of TLR-7/8a with HEK293 cells expressing human TLR-7 and a reporter enzyme, SEAP (InvivoGen cat #hkb-htlr7). R848 ("Resiquimod") is shown for comparison. (**b**,**c**) C57BL/6 mice (*n* = 5 per group) were injected subcutaneously with either (**b**) the Adpgk minimal epitope (ASMTNMELM) or (**c**) a model CD4 T cell epitope (AKFVAAWTLKAAA, "PADRE") as charge-modified (CM) conjugates comprising different compositions of oligo-7/8a. Blood was collected on day 22 and assessed for IFN-γ-producing T cells by intracellular cytokine staining. Data on log scale are reported as geometric mean with 95% c.i.

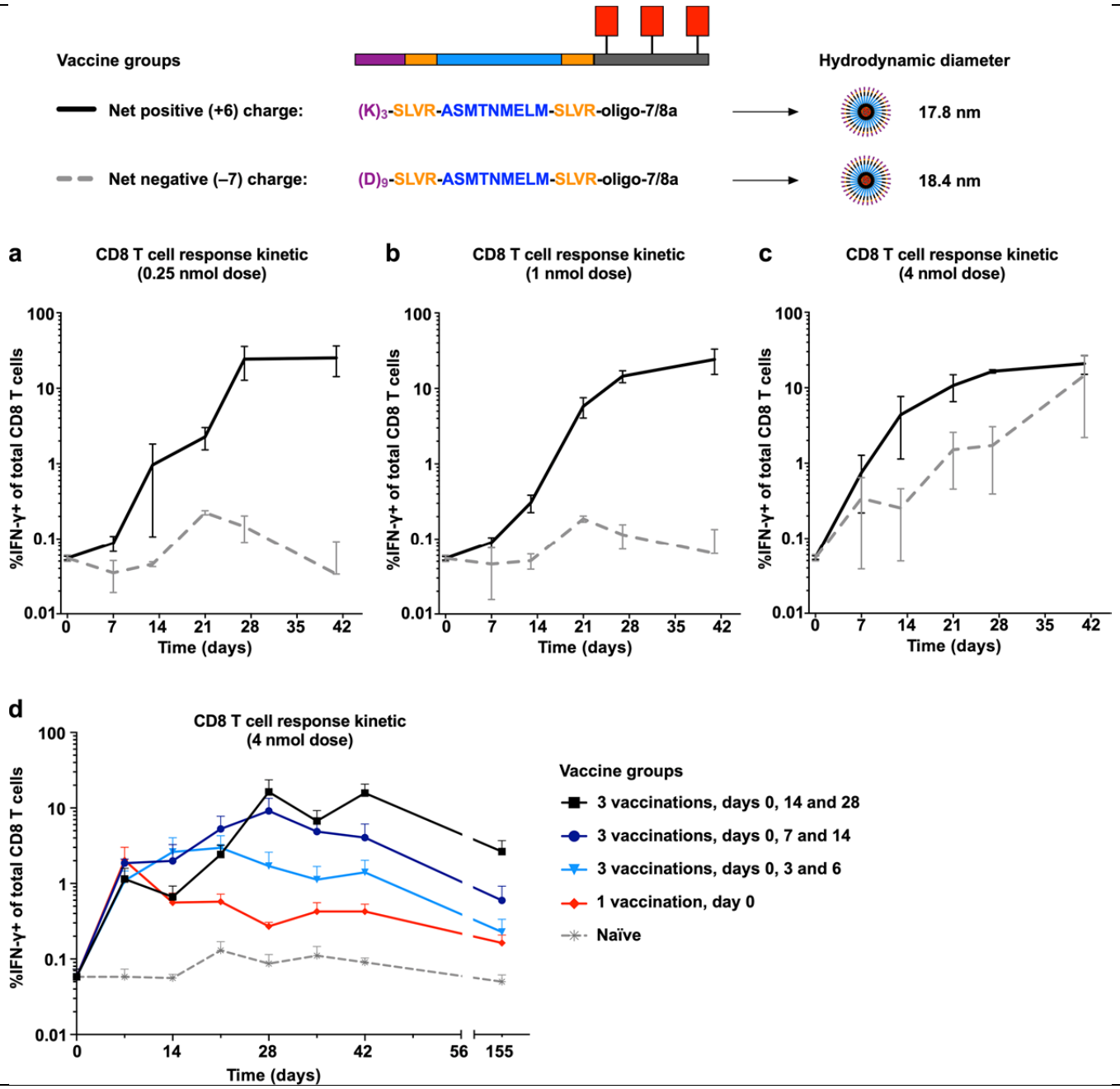

Supplementary Figure 6

Impact of net charge and vaccine regimen on CD8 T cell responses.

(**a**–**c**) An MHC-I (H-2D^b)-restricted epitope (ASMTNMELM) from the MC38 tumor cell line derived neoantigen, Adpgk, was prepared as a charged-modified (CM) conjugate with either net positive (+6) or net negative (–7) charge. The positive and negatively charged CM conjugates were administered subcutaneously to mice (*n* = 3 per group per dose) at days 0, 14 and 28 at doses of either (**a**) 0.25 nmol, (**b**) 1 nmol or (**c**) 4 nmol per vaccination, and CD8 T cell responses from blood were evaluated by intracellular cytokine staining at the time points shown. (**d**) The LP neoantigen Adpgk as SNP-7/8a based on a CM conjugate with net positive charge was subcutaneously administered at 4 nmol per dose to C57BL/6 mice (*n* = 3 per group) either once (1 vaccination) or 3 times with either 3, 7 or 14 days between immunizations. CD8 T cell responses were assessed by intracellular cytokine staining at the time points shown. Data are reported as mean ± s.e.m.

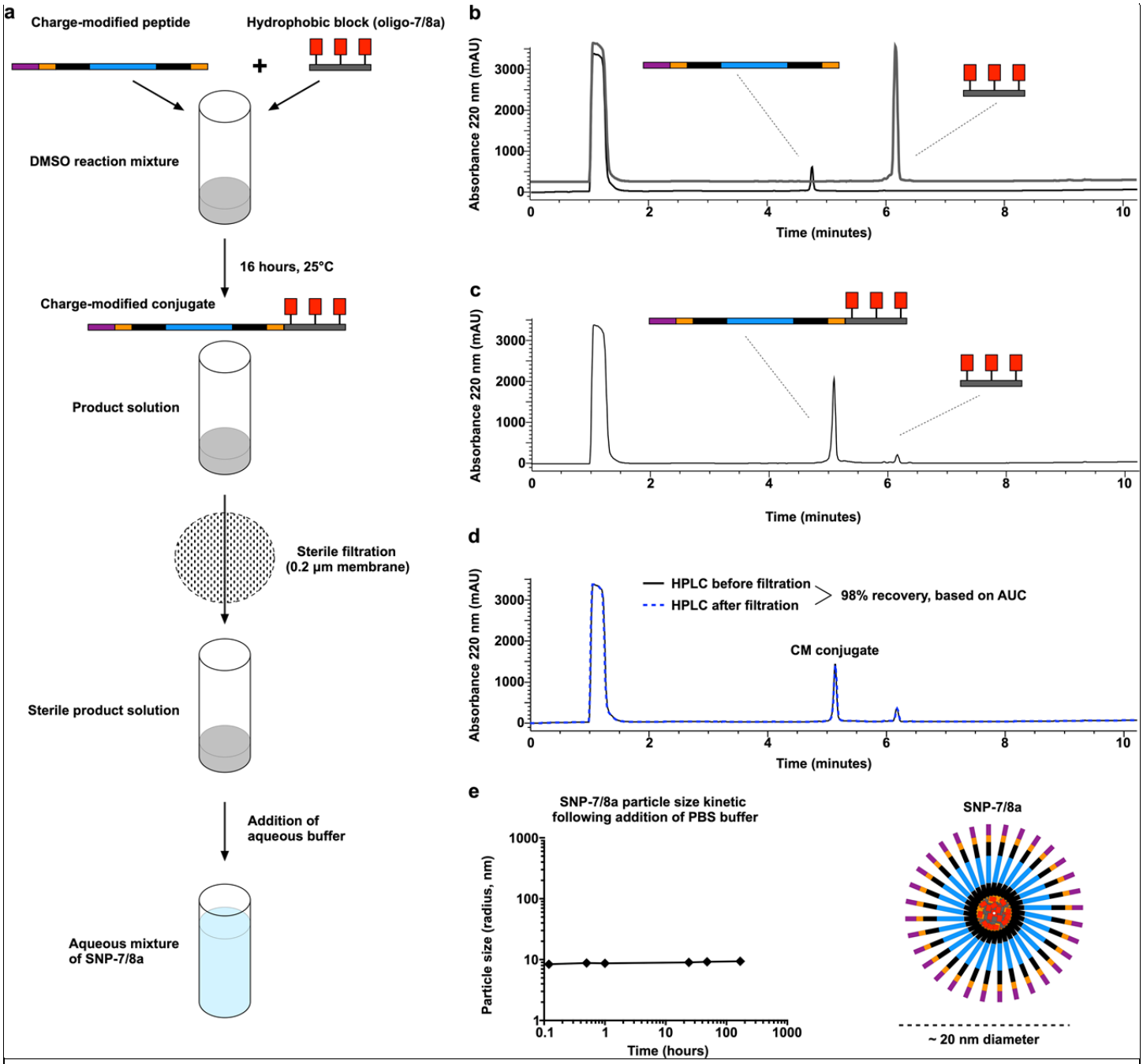

Supplementary Figure 7

Manufacturing workflow for PCVs based on SNP-7/8a.

(**a**) Schematic of the manufacturing workflow for production of a PCV. Each CM peptide comprises a patient-specific neoantigen and is produced on-demand by solid-phase peptide synthesis. The hydrophobic block (oligo-7/8a) is the same for each patient and manufactured in bulk. Each patient-specific CM peptide is reacted with the oligo-7/8a in DMSO at room temperature for 16 hours to yield a CM conjugate product solution. The product solution is sterile filtered to produce a sterile product solution. Addition of aqueous buffer to the sterile product solution results in the CM conjugates self-assembling into nanoparticles. (**b**) Representative HPLC chromatograms of a CM peptide and oligo-7/8a. Representative HPLC chromatograms of a product solution (**c**) and sterile product solution (**d**). Overlaying the chromatogram prior to and after sterile filtration indicates that no significant change in composition has occurred. (**e**) SNP-7/8a particle size over time following addition of PBS, pH 7.4 to a sterile product solution comprising a CM

conjugate.

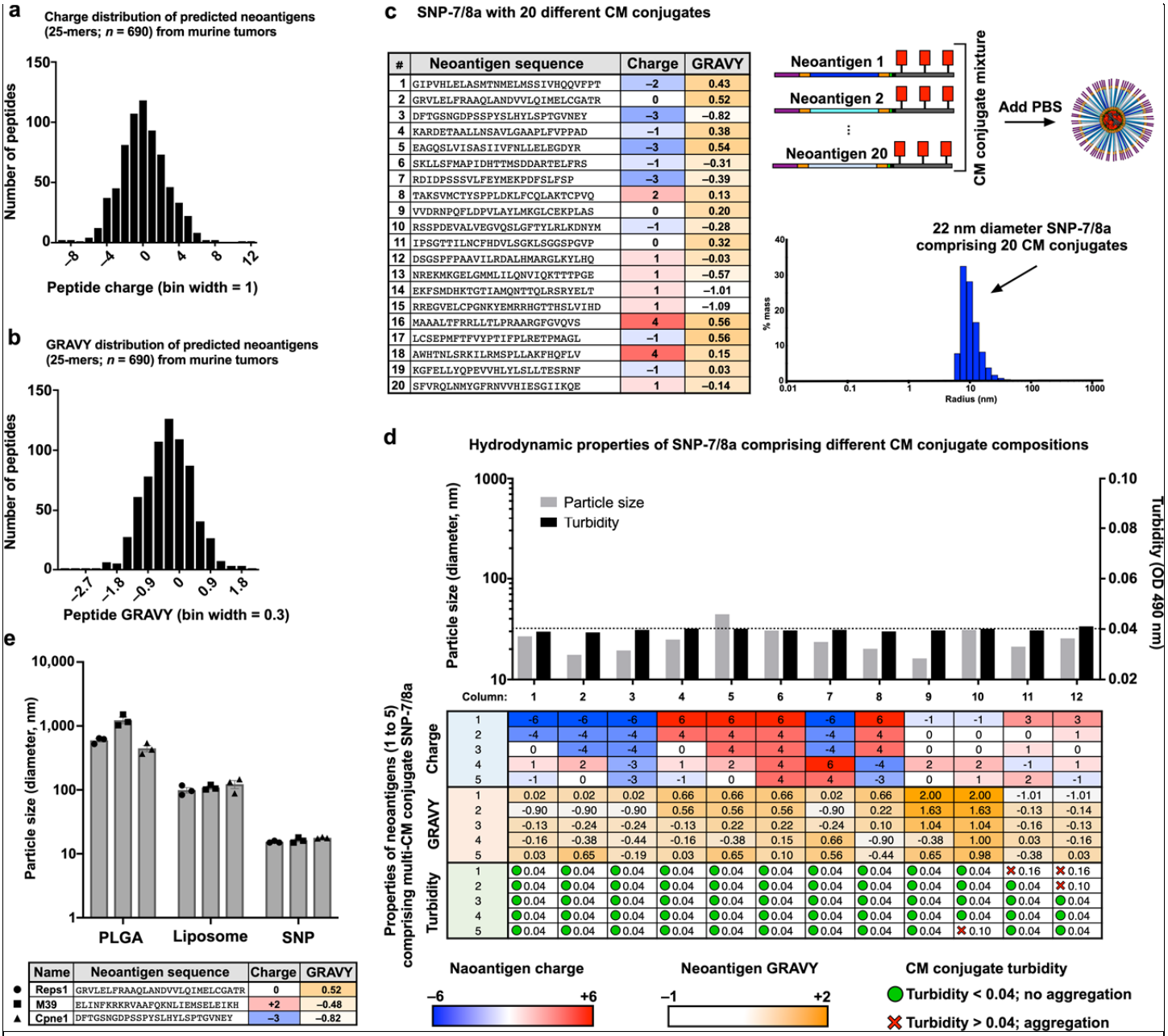

#	Neoantigen sequence	Charge	GRAVY
1	GIPVHLELASMTNMELMSSIVHQQVFPT	–2	0.43
2	GRVLELFRAAQLANDVVLQIMELCGATR	0	0.52
3	DFTGSNGDPSSPYSLHYLSPTGVNEY	–3	–0.82
4	KARDETAALLNSAVLGAAPLFVPPAD	–1	0.38
5	EAGQSLVISASIIVFNLLELEGDYR	–3	0.54
6	SKLLSFMAPIDHTTMSDDARTELFRS	–1	–0.31
7	RDIDPSSSVLFEYMEKPDFSLFSP	–3	–0.39
8	TAKSVMCTYSPPLDKLFCQLAKTCPVQ	2	0.13
9	VVDRNPQFLDPVLAYLMKGLCEKPLAS	0	0.20
10	RSSPDEVALVEGVQSLGFTYLRLKDNYM	–1	–0.28
11	IPSGTTILNCFHDVLSGKLSGGSPGVP	0	0.32
12	DSGSPFFPAAVILRDALHMARGLKYLHQ	1	–0.03
13	NREKMKGELGMMLILQNVIQKTTTPGE	1	–0.57
14	EKFSMDHKTGTIAMQNTTQLRSRYELT	1	–1.01
15	RREGVELCPGNKYEMRRHGTTHSLVIHD	1	–1.09
16	MAAALTFRRLLTLPRAARGFGVQVS	4	0.56
17	LCSEPMFTFVYPTIFPLRETPMAGL	–1	0.56
18	AWHTNLSRKILRMSPLLAKFHQFLV	4	0.15
19	KGFELLYQPEVVHLYLSLLTESRNF	–1	0.03
20	SFVRQLNMYGFRNVVHIESGIIKQE	1	–0.14

	Name	Neoantigen sequence	Charge	GRAVY
●	Reps1	GRVLELFRAAQLANDVVLQIMELCGATR	0	0.52
■	M39	ELINFKRKRVAAFQKNLIEMSELEIKH	+2	–0.48
▲	Cpne1	DFTGSNGDPSSPYSLHYLSPTGVNEY	–3	–0.82

		1	2	3	4	5	6	7	8	9	10	11	12
1	Charge	-6	-6	-6	6	6	6	-6	6	-1	-1	3	3
2		-4	-4	-4	4	4	4	-4	4	0	0	0	1
3		0	-4	-4	0	4	4	-4	4	0	0	1	0
4		1	2	-3	1	2	4	6	-4	2	2	-1	1
5		-1	0	-3	-1	0	4	4	-3	0	1	2	-1
1	GRAVY	0.02	0.02	0.02	0.66	0.66	0.66	0.02	0.66	2.00	2.00	-1.01	-1.01
2		-0.90	-0.90	-0.90	0.56	0.56	0.56	-0.90	0.22	1.63	1.63	-0.13	-0.14
3		-0.13	-0.24	-0.24	-0.13	0.22	0.22	-0.24	0.10	1.04	1.04	-0.16	-0.13
4		-0.16	-0.38	-0.44	-0.16	-0.38	0.15	0.66	-0.90	-0.38	1.00	0.03	-0.16
5		0.03	0.65	-0.19	0.03	0.65	0.10	0.56	-0.44	0.65	0.98	-0.38	0.03
1	Turbidity	0.04	0.04	0.04	0.04	0.04	0.04	0.04	0.04	0.04	0.04	0.16	0.16
2		0.04	0.04	0.04	0.04	0.04	0.04	0.04	0.04	0.04	0.04	0.04	0.10
3		0.04	0.04	0.04	0.04	0.04	0.04	0.04	0.04	0.04	0.04	0.04	0.04
4		0.04	0.04	0.04	0.04	0.04	0.04	0.04	0.04	0.04	0.04	0.04	0.04
5		0.04	0.04	0.04	0.04	0.04	0.04	0.04	0.04	0.04	0.10	0.04	0.04

Supplementary Figure 8

SNP-7/8a can accommodate multiple CM conjugates comprising predicted neoantigens with variable charge and hydropathy.

(**a**) Charge and (**b**) grand average of hydropathy (GRAVY) distribution plots for *n* = 690 LP neoantigens derived from 3 mouse tumor models (B16-F10, MC38 and SB-3123). (**c**) Table listing the properties of 20 different predicted neoantigens that were synthesized as CM conjugates and then mixed at equimolar ratios in DMSO followed by addition of PBS buffer to generate SNP-7/8a consisting of 20 different CM conjugates. (**d**) Particle size and turbidity of SNP-7/8a consisting of different CM conjugate compositions. The bar charts show the particle size (gray bars; left axis) and turbidity (black bars; right axis) of 12 SNP-7/8a formulations, each containing a unique set of 5 different CM conjugates. The properties of the CM conjugates are listed in the accompanying table. Each column lists the charge and GRAVY characteristics of the neoantigens comprising each of the 5 CM conjugates as well as the turbidity measured for the 5 CM conjugates when each are individually resuspended in PBS. For example, column 1 shows the size and turbidity of a particle (SNP-7/8a) comprised of 5 different CM conjugates; the 5 CM conjugates (1 through 5) are comprised of neoantigens with a net charge of –6, –4, 0, +1, and –1 and GRAVY of 0.02, –0.90, –0.13, –0.16, 0.03; and, those CM conjugates (1 through 5) each have turbidity < 0.04. In columns 10–12, CM conjugates that individually are prone to form aggregates incorporate into stable nanoparticle micelles

when formulated with other CM conjugates that individually form stable nanoparticle micelles. (**e**) Different predicted neoantigens (Reps1, M39 and Cpne1) were formulated as either PLGA microparticles, liposomal particles or SNP-7/8a, and the sizes of the particulate formulations were assessed by dynamic light scattering. Data are reported as mean ± s.e.m.

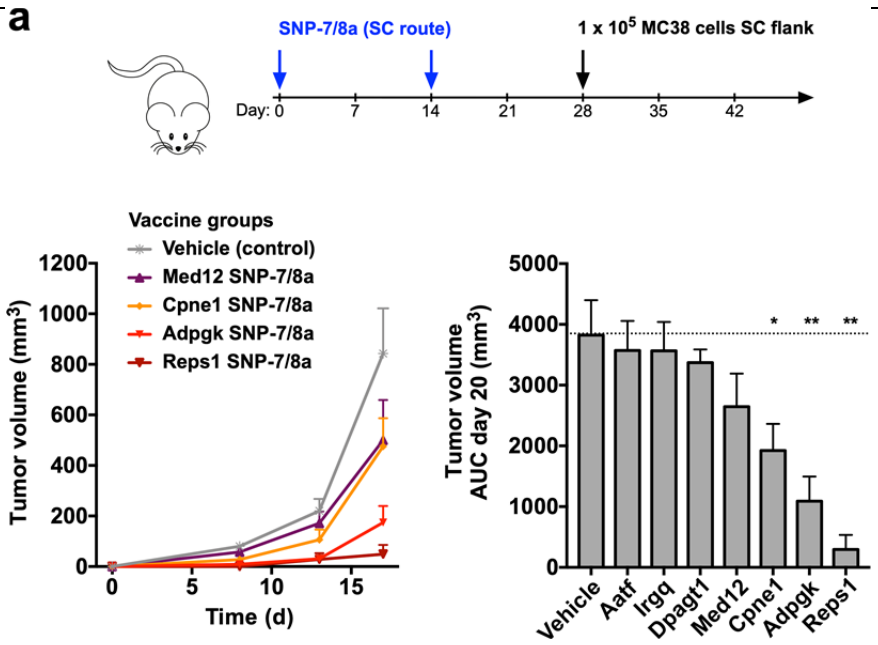

Supplementary Figure 9

Anti-tumor efficacy of SNP-7/8a delivering MC38 neoantigens.

(**a**) C57BL/6 mice (*n* = 10 per group) were vaccinated subcutaneously with SNP-7/8a including different MC38 LP neoantigens or vehicle control (10% DMSO in PBS) on days 0 and 14. On day 28, mice were subcutaneously implanted with 1.0×10^5 MC38 tumor cells. Tumor growth curves (left) and area under the curve through day 20 (right) are shown. Data on linear scale are reported as mean ± s.e.m. Statistical significance was determined using Kruskal-Wallis with Dunn's correction; ns = not significant, $^*P < 0.05$, $^{**}P \leq 0.01$.

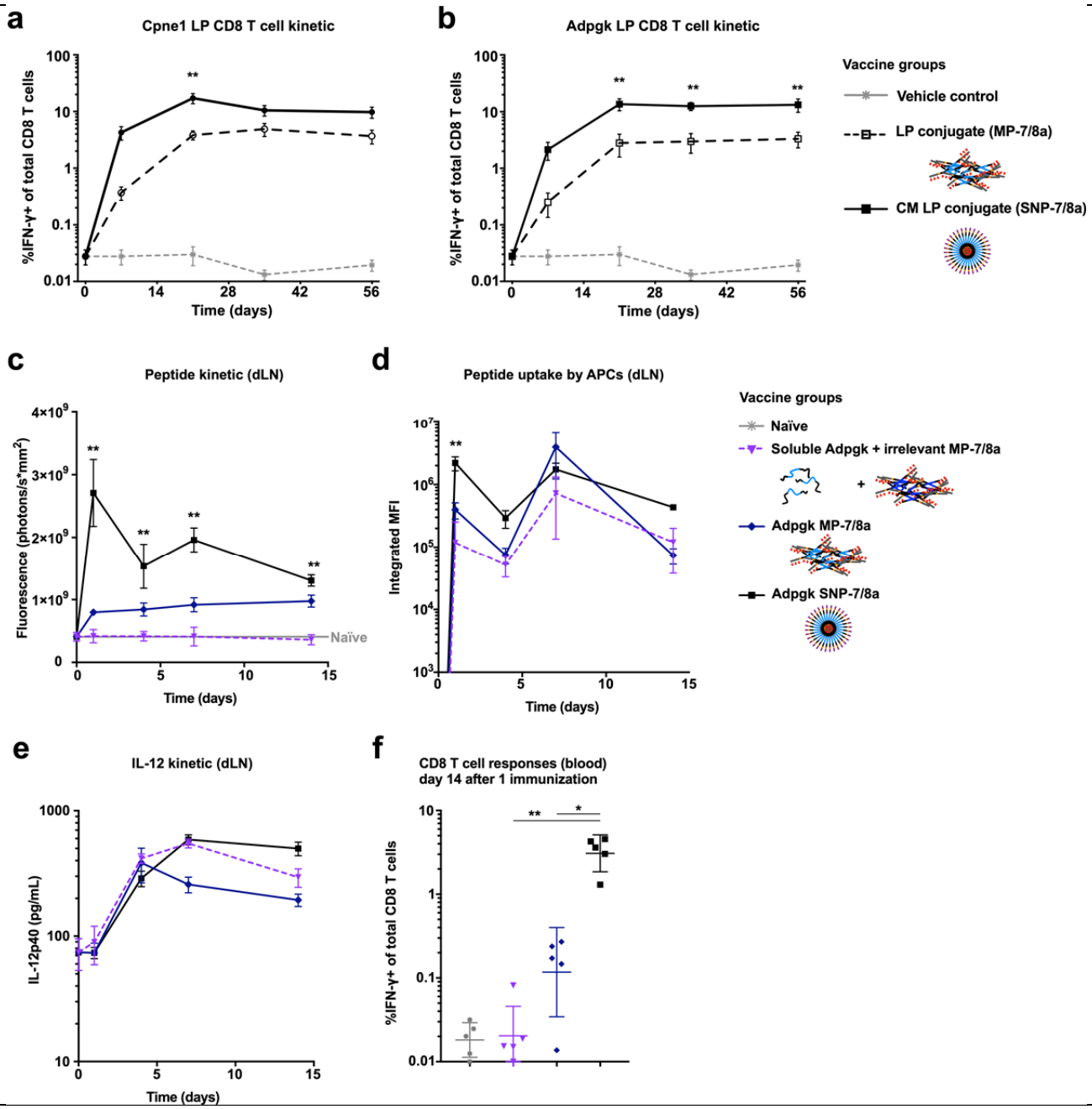

Supplementary Figure 10

SNP-7/8a leads to higher magnitude CD8 T cell responses and more antigen uptake by lymph node APCs than MP-7/8a.

(**a,b**) C57BL/6 mice (*n* = 5 per group) were injected subcutaneously with either (**a**) Cpne1 LP or (**b**) Adpgk LP as MP-7/8a or SNP-7/8a on days 0, 14 and 28 and CD8 T cell responses were assessed by intracellular cytokine staining at various time points. (**c–f**) C57BL/6 mice (*n* = 5 per group per time point) were immunized with AF647-labeled Adpgk Min either as the soluble peptide admixed with MP-7/8a containing an irrelevant antigen, as MP-7/8a or as SNP-7/8a. Lymph nodes draining the site of immunization were collected at serial time points and assessed for (**c**) total tissue fluorescence (peptide quantity), (**d**) antigen uptake by APCs and (**e**) IL-12p40 cytokine production. (**f**) CD8 T cell responses from blood were assessed by intracellular cytokine staining on day 14. Data on log scale are reported as geometric mean with 95% c.i., except line graphs are reported as mean ± s.e.m. Statistical significance was determined using ANOVA with Bonferroni correction; ns = not significant, **P* < 0.05, ***P* ≤ 0.01.

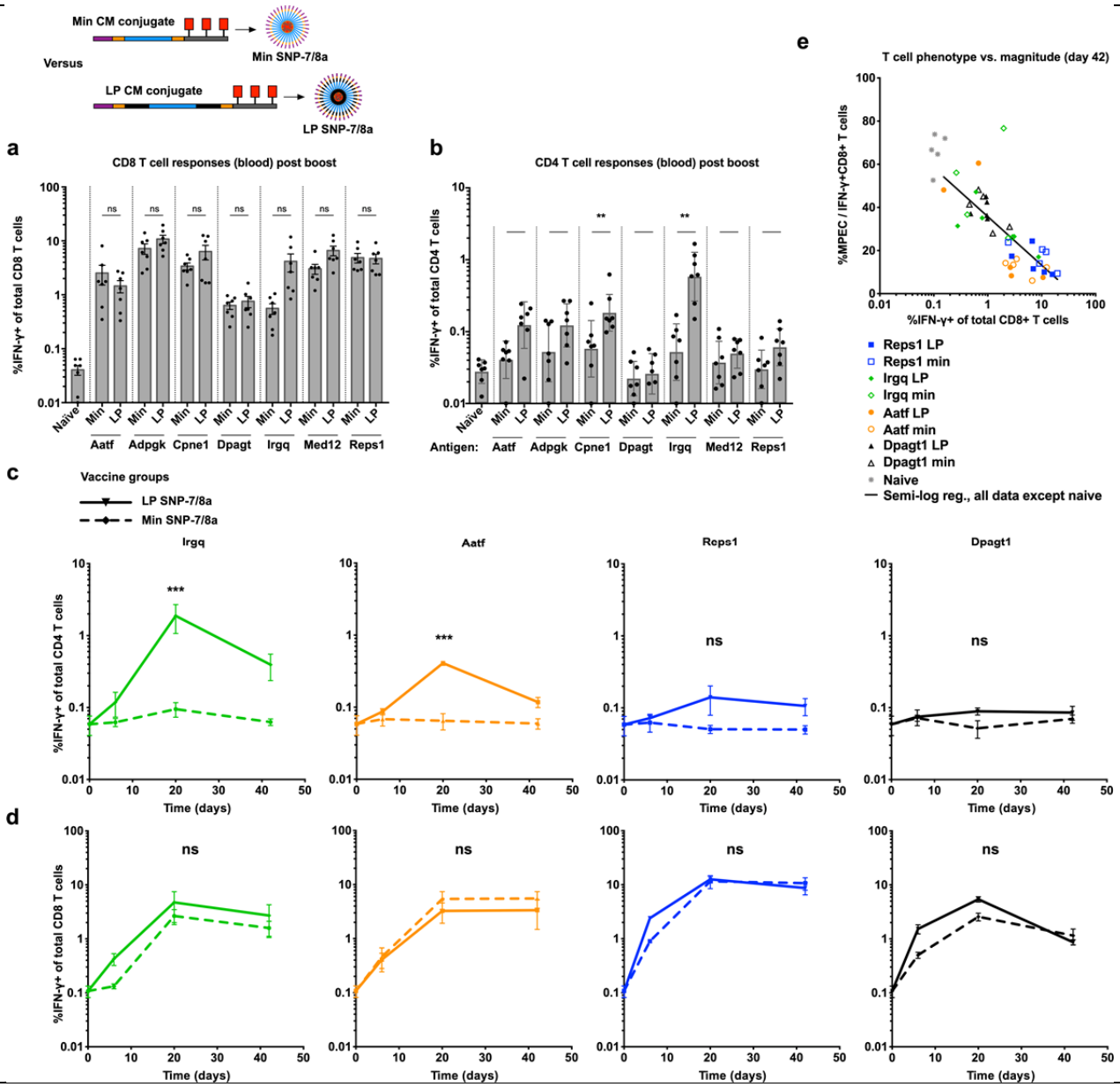

Supplementary Figure 11

Effect of peptide antigen length on CD8 and CD4 T cell responses.

(**a,b**) C57BL/6 mice (*n* = 5) were vaccinated subcutaneously on days 0 and 14 with either the short or long (Min or LP) version of one of 7 different MC38 neoantigens formulated as SNP-7/8a. (**a**) CD8 and (**b**) CD4 T cell responses from blood were determined by intracellular cytokine staining on day 21. (**c**–**e**) C57BL/6 mice (*n* = 5) were vaccinated subcutaneously on days 0 and 14 with either the short or long (Min or LP) version of Irgq, Aatf, Reps1 and Dpagt1, wherein the LP versions contain a CD4 epitope that results in high, moderate, low or no detectable CD4 T cell responses, respectively. (**c**) CD8 T cell responses and (**d**) CD4 T cell responses were assessed by intracellular cytokine staining on days 7, 21 and 42. While CD4 T cell responses are detected in the LP version for certain antigens, no differences in the magnitude or kinetic of CD8 T responses were observed between groups of mice immunized with the LP or Min. (**e**) Evaluation of the phenotype of CD8 T cell responses as assessed by the % of antigen-specific (IFN-γ+) CD8 T cells that display a memory precursor effector cell (MPEC) phenotype (KLRG1^{low}CD127^{high}) shows that there are no differences in the proportion of memory and effector CD8 T cells elicited by the LP as compared with the Min when delivered as SNP-7/8a. Data on log scale are reported as geometric mean with 95% c.i., except data on line graphs are reported as mean ± s.e.m. Statistical significance was determined using two-way ANOVA with Bonferroni correction; ns = not significant, **P* < 0.05, ***P* ≤ 0.01.

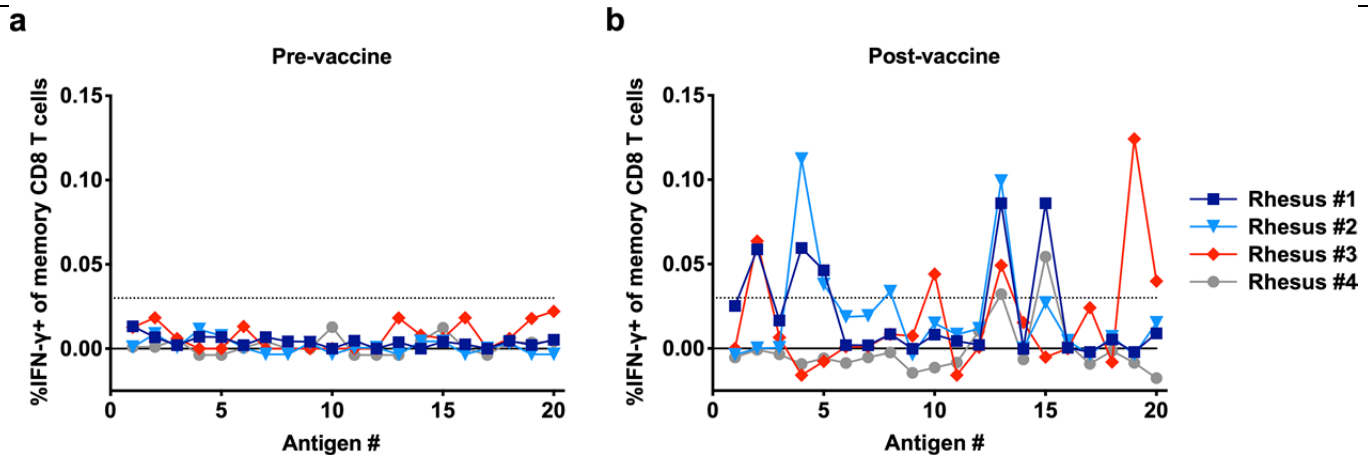

Supplementary Figure 12

CD8 T cell responses to individual antigens following SNP-7/8a vaccination in primates.

(**a**,**b**) Paired pre- and post-vaccine PBMC samples were stimulated with each individual peptide antigen included in the SNP-7/8a vaccine or a control antigen (specifically, a mock neoantigen that had not been included in the vaccine) without prior *ex vivo* expansion and assessed by intracellular cytokine staining. Antigen-specific CD8 T cell responses to each antigen are reported for (**a**) pre-vaccine PBMC and (**b**) post-vaccine PBMC after subtracting the response to the control antigen (the assay background). An IFN-γ response threshold of 0.03% is shown by the dotted line. No rhesus had a response to any antigen above the threshold in the pre-vaccine samples. In the post-vaccine samples, the number of antigens to which the rhesus had a CD8 T cell response above the threshold were 5, 4, 5, and 2 for rhesus #1 through #4, respectively.

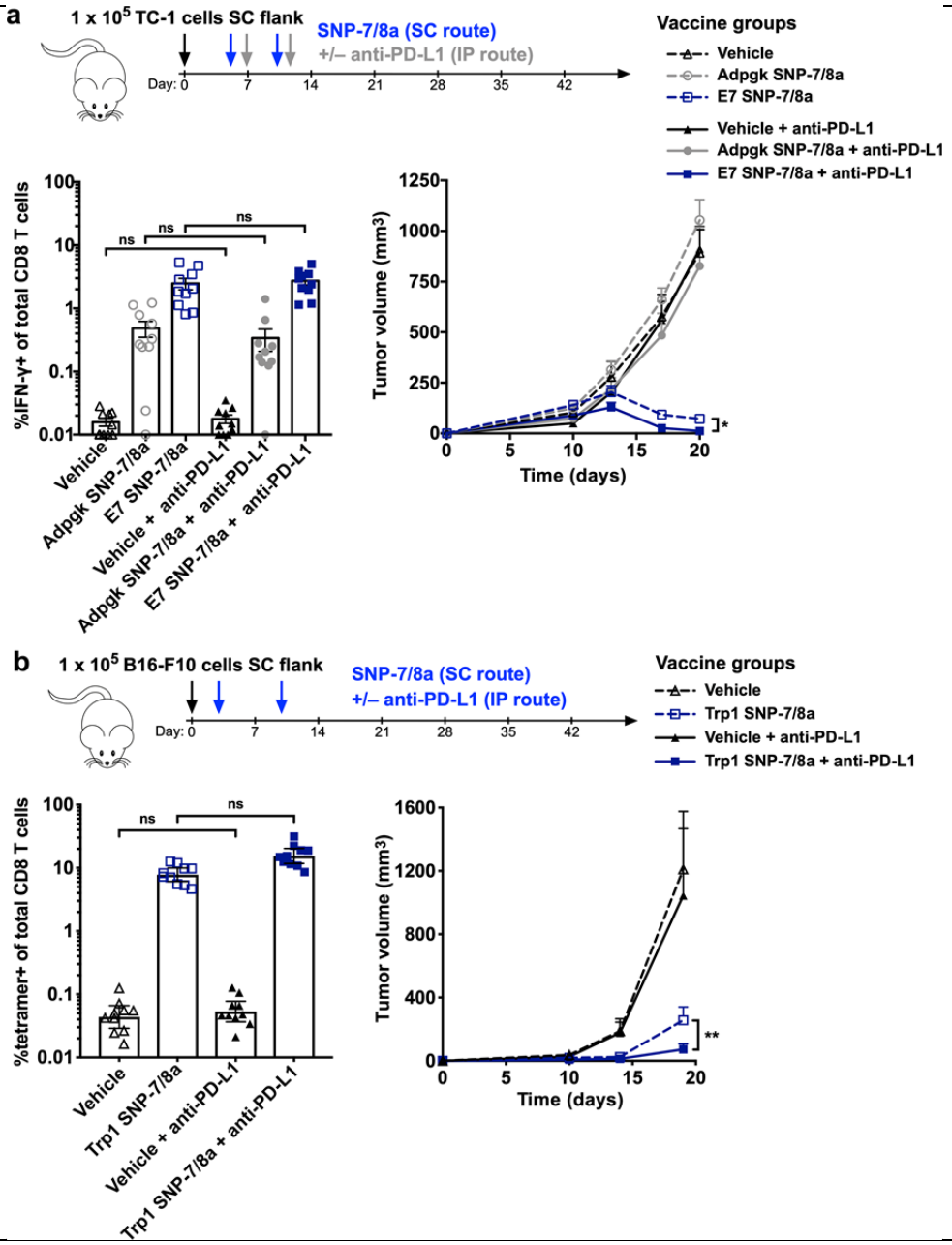

Supplementary Figure 13

Effect of checkpoint inhibitor on therapeutic efficacy with SNP-7/8a.

(**a**) C57BL/6 mice (n = 20 per group) implanted with 1.0×10^5 TC-1 tumor cells were vaccinated subcutaneously (SC) either with vehicle control (10% DMSO in PBS), SNP-7/8a delivering E7 from human papilloma virus or an irrelevant antigen (Adpgk neoantigen from MC38) as an inflammation control on days 5 and 10 after implantation. Half the animals from each group (n = 10) were treated with 200 μg anti-PD-L1 administered intraperitoneal (IP) on days 7 and 12 after implantation. CD8 T cell responses on day 12 (left) and tumor growth curves (right) are shown. (**b**) C57BL/6 mice (n = 20 per group) implanted with 1.0×10^5 B16-F10 tumor cells were vaccinated SC either with vehicle control (10% DMSO in PBS) or SNP-7/8a delivering Trp1 self-antigen on days 3 and 10 after implantation. Half the animals from each group (n = 10) were treated with 200 μg anti-PD-L1 administered IP concomitant with vaccination on days 3 and 10. CD8 T cell responses on day 12 (left) and tumor growth curves (right) are shown. Data on log scale are reported as geometric mean with 95% c.i.; data on linear scale are reported as mean ± s.e.m. Statistical significance was determined using one-way or two-way ANOVA with Bonferroni correction; ns = not significant, *P < 0.05, **P ≤ 0.01.

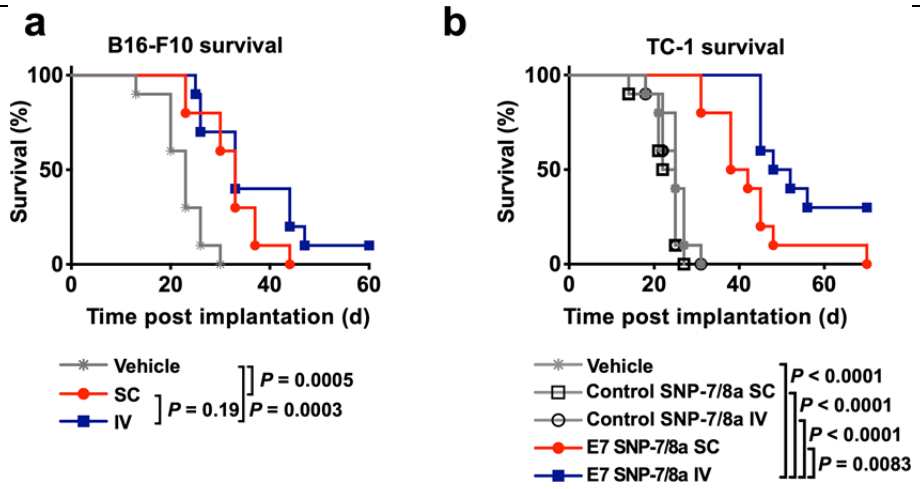

Supplementary Figure 14

IV administration of SNP-7/8a mediates tumor regression.

(**a**) C57BL/6 mice (*n* = 10 per group) implanted subcutaneously with 1.0×10^5 B16-F10 tumor cells were treated with either SNP-7/8a delivering the self-antigen Trp1 by the SC or IV route, or vehicle control (DMSO/PBS) by the IV route, which were each given along with anti-PD-L1 by the IP route on days 3, 10 and 17. Tumor growth was monitored at various time points. (**b**) C57BL/6 mice (*n* = 10 per group) implanted subcutaneously with 1.0×10^5 TC-1 tumor cells were treated with either vehicle control (DMSO/PBS) by the IV route, or SNP-7/8a delivering the virus-associated tumor antigen HPV E7 or an irrelevant antigen (Adpgk neoantigen from MC38) as an inflammation control ("control SNP-7/8a") by the SC or IV route. Treatments were given along with anti-PD-L1 delivered by the IP route on days 7 and 14. Tumor growth was monitored at various time points. Statistical significance was determined by log-rank test.

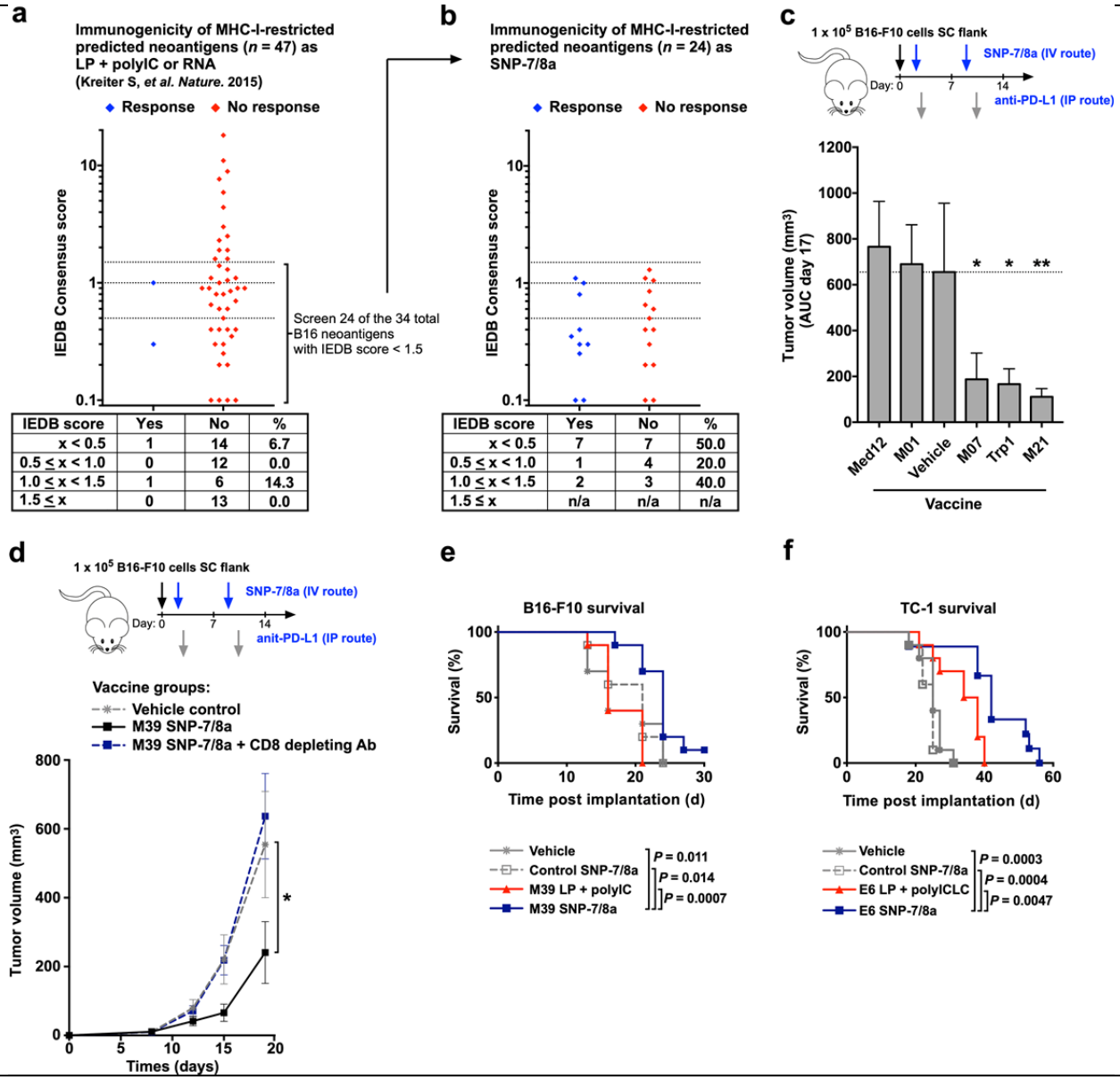

IEDB score	Yes	No	%
x < 0.5	1	14	6.7
0.5 ≤ x < 1.0	0	12	0.0
1.0 ≤ x < 1.5	1	6	14.3
1.5 ≤ x	0	13	0.0

IEDB score	Yes	No	%
x < 0.5	7	7	50.0
0.5 ≤ x < 1.0	1	4	20.0
1.0 ≤ x < 1.5	2	3	40.0
1.5 ≤ x	n/a	n/a	n/a

Supplementary Figure 15

Immunogenicity and anti-tumor efficacy of SNP-7/8a.

(**a**) Plot of the predicted MHC-I binding affinity (IEDB consensus, any length, H2-K^b or H2-D^b) versus CD8 T cell response for B16-F10 neoantigens (*n* = 47) included in PCVs based on LP + polyIC or RNA as described (see: Kreiter S, *et al. Nature*, 520; 692–696, 2015). (**b**) 24 of the predicted neoantigens from panel (**a**) with moderate to high MHC-I binding affinity (IEDB consensus score < 1.5) were screened for immunogenicity *in vivo* using SNP-7/8a and the relationship between binding affinity and immunogenicity is shown. (**c**) C57BL/6 mice (*n* = 10 per group) implanted subcutaneously with 1 × 10^5 B16-F10 cells were treated with vehicle control (DMSO/PBS) or SNP-7/8a containing either one of 4 B16-F10 LP neoantigens (M01, M07, M21 or M39), Trp1 self-antigen (positive control) or an irrelevant neoantigen (Med12 neoantigen from MC38) as an inflammation control by the IV route on days 1 and 8. All animals also received 200 μg anti-PD-L1 by the IP route on the days indicated. (**c**) Area under the curve of tumor growth is shown for animals vaccinated with SNP-7/8a delivering the indicated antigens. (**d**) C57BL/6 mice (*n* = 10 per group) implanted subcutaneously with 1 × 10^5 B16-F10 cells were treated with vehicle control (DMSO/PBS) or M39 SNP-7/8a by the IV route on days 1 and 8. An additional group of mice (*n* = 10) treated with M39 SNP-7/8a was conditioned with CD8 depleting antibody (250 μg IP) prior to treatment. All animals also received 200 μg anti-PD-L1 by the IP route on the days indicated. Tumor growth curves are shown (**e**) C57BL/6 mice (*n* = 10 per group) implanted subcutaneously with 1.0 × 10^5 B16-F10 tumor cells were treated with either the M39 neoantigen as LP

admixed with polyIC by the SC route, M39 as SNP-7/8a by the IV route, an irrelevant neoantigen (Adpgk) as SNP-7/8a ("control SNP-7/8a") by the IV route or vehicle control (DMSO/PBS) by the IV route. Treatments were given along with anti-PD-L1 delivered by the IP route on days 1,8 and 15. Tumor growth was monitored at various time points. (**f**) C57BL/6 mice (*n* = 10 per group) implanted subcutaneously with 1.0×10^5 TC-1 tumor cells were treated with either the virus-associated tumor antigen HPV E6 as an LP admixed with polyICLC by the SC route, E6 as SNP-7/8a by the IV route, an irrelevant neoantigen (Adpgk) as SNP-7/8a by the IV route ("control SNP-7/8a"); or, vehicle control (DMSO/PBS) by the IV route. Treatments were given along with anti-PD-L1 delivered by the IP route on days 7 and 14. Tumor growth was monitored at various time points and survival curves are shown. Data on linear scale are reported as mean ± s.e.m. Statistical significance was determined using Kruskal-Wallis with Dunn's correction (**c**), two-way ANOVA with Bonferroni correction (**d**) or log-rank test (**e**,**f**); ns = not significant, $*P < 0.05$, $**P \leq 0.01$.